

iScience, Volume 27

Supplemental information

Lysosomal stress drives the release of pathogenic α -synuclein from macrophage lineage cells via the LRRK2-Rab10 pathway

Tetsuro Abe, Tomoki Kuwahara, Shoichi Suenaga, Maria Sakurai, Sho Takatori, and Takeshi Iwatsubo

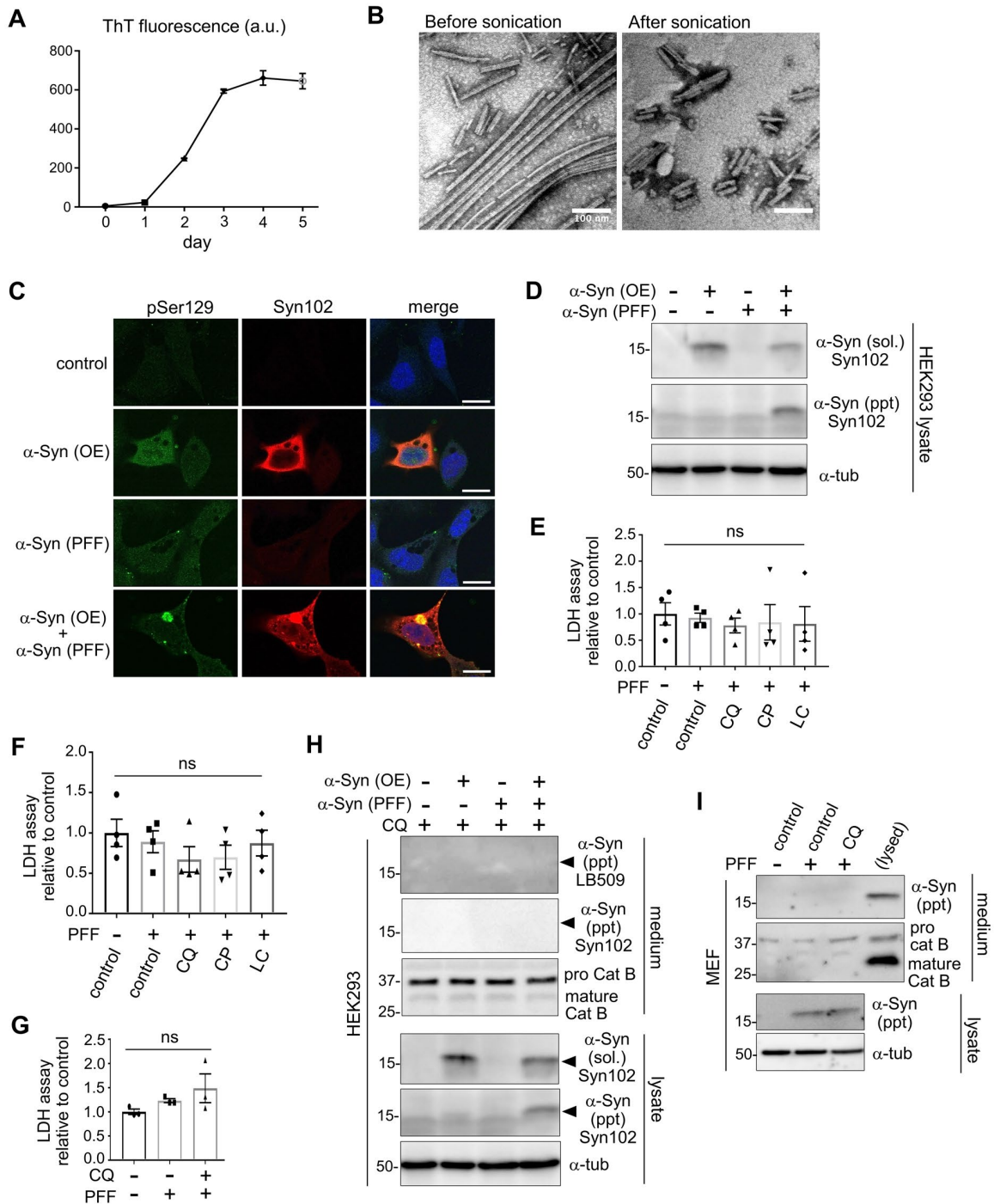


Figure S1. Characterization of α -synuclein preformed fibrils (PFFs) generated in this study, related to Figure 1.

(A) Evaluation of fibril formation of recombinant α -synuclein by Thioflavin T fluorescence assay. The fluorescence increased with incubation time. Data represent mean \pm SD of duplicate samples. **(B)** Negative electron microscopic visualization of recombinant α -synuclein fibrils before (left) and after (right) sonication. Scale bar = 100 nm. **(C)** Assessment of seeding activity of generated PFFs

by immunocytochemistry. Treatment of HEK293 cells with PFFs in addition to overexpression (OE) of α -synuclein induced the formation of phospho-Ser129- α -synuclein positive intracellular aggregates. Bars = 15 μ m. **(D)** Biochemical confirmation of seeding activity of PFFs by immunoblotting. Addition of α -synuclein PFFs to HEK293 cells produced 1% Triton X-100 insoluble (ppt) α -synuclein only in the presence of overexpressed (OE) α -synuclein. **(E-G)** The measurements of LDH activity in media from RAW264.7 cells (E), MG6 cells (F) or mouse primary microglia (G). ns: not significant. **(H, I)** Lack of the release of insoluble α -synuclein and mature cathepsin B from CQ-treated mouse embryonic fibroblasts (MEF) (H) or HEK293 cells pretreated with α -synuclein PFFs and/or α -synuclein overexpression (OE) (I).

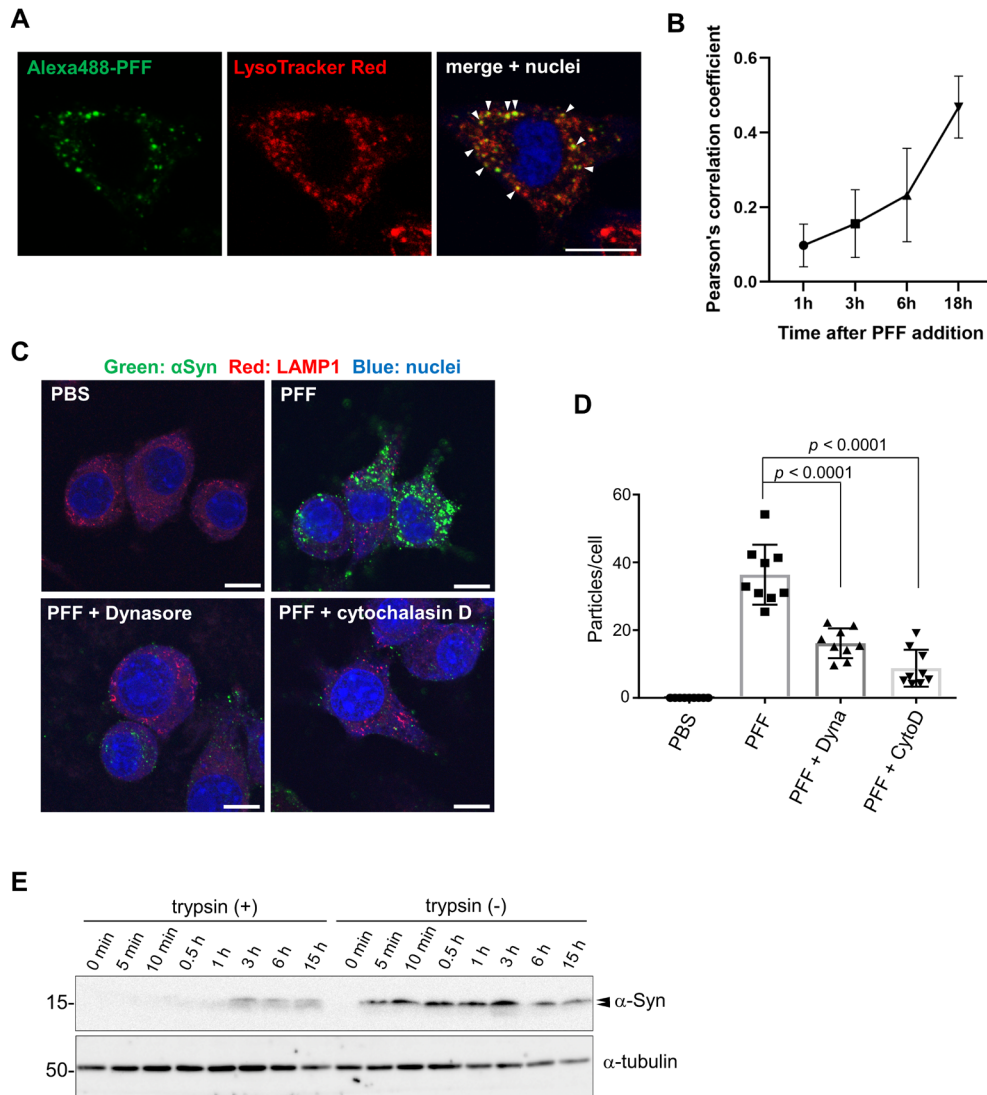


Figure S2. Confirmation of the internalization of α -synuclein PFFs and the effect of trypsin on the removal of cell surface α -synuclein, related to Figure 2.

(A) Colocalization of internalized Alexa488-labeled α -synuclein PFFs with LysoTracker Red in RAW264.7 cells. Representative fluorescence images 18 hrs after addition of Alexa488-PFFs are shown. Arrowheads indicate the sites of colocalization. Bar = 10 μ m. **(B)** Time-dependent increase of colocalization of Alexa488-PFFs and LysoTracker Red, as calculated by Pearson's correlation coefficient. Data represent mean \pm S.D., $n = 20$ fields each. **(C)** Confirmation of the inhibitory effect of Dynasore and cytochalasin D on the 3-hr uptake of α -synuclein PFFs by immunocytochemistry. Bars = 10 μ m. **(D)** Quantification of the internalized α -synuclein particles, as shown in C. Data represent mean \pm SEM, $n = 9$, one-way ANOVA with Tukey's test. **(E)** Immunoblot analysis of α -synuclein in the lysates of RAW264.7 cells that were exposed to α -synuclein PFFs for the indicated times followed by the treatment with or without trypsin before collecting cells.

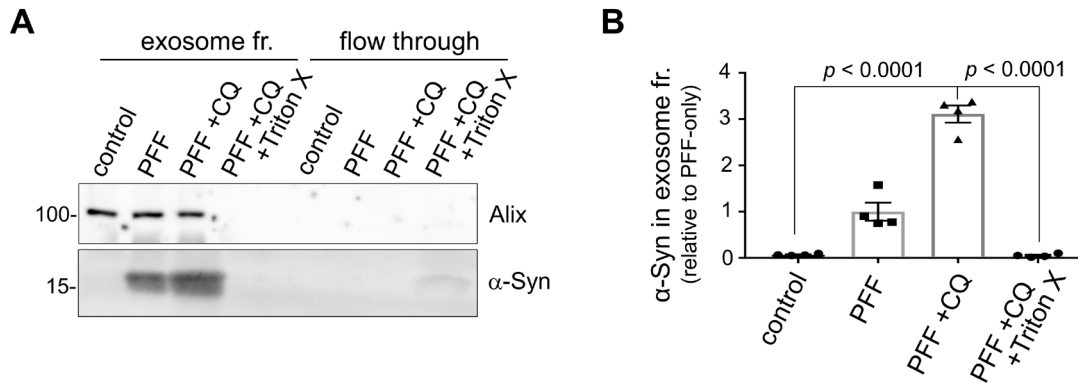


Figure S3. Release of α -synuclein into the exosomal fraction in microglial MG6 cells, related to Figure 3.

(A) Representative immunoblot pictures of α -synuclein and Alix in exosomal and flow-through fractions of media from MG6 cells that were treated as indicated. Exosomes are isolated with ultracentrifugation-free method using magnetic beads, as shown in Figure 3B. Triton X-100 was treated just prior to exosome isolation. **(B)** Quantification of α -synuclein in the exosome fraction. Mean \pm SEM, $n = 4$, one-way ANOVA with Tukey's test.

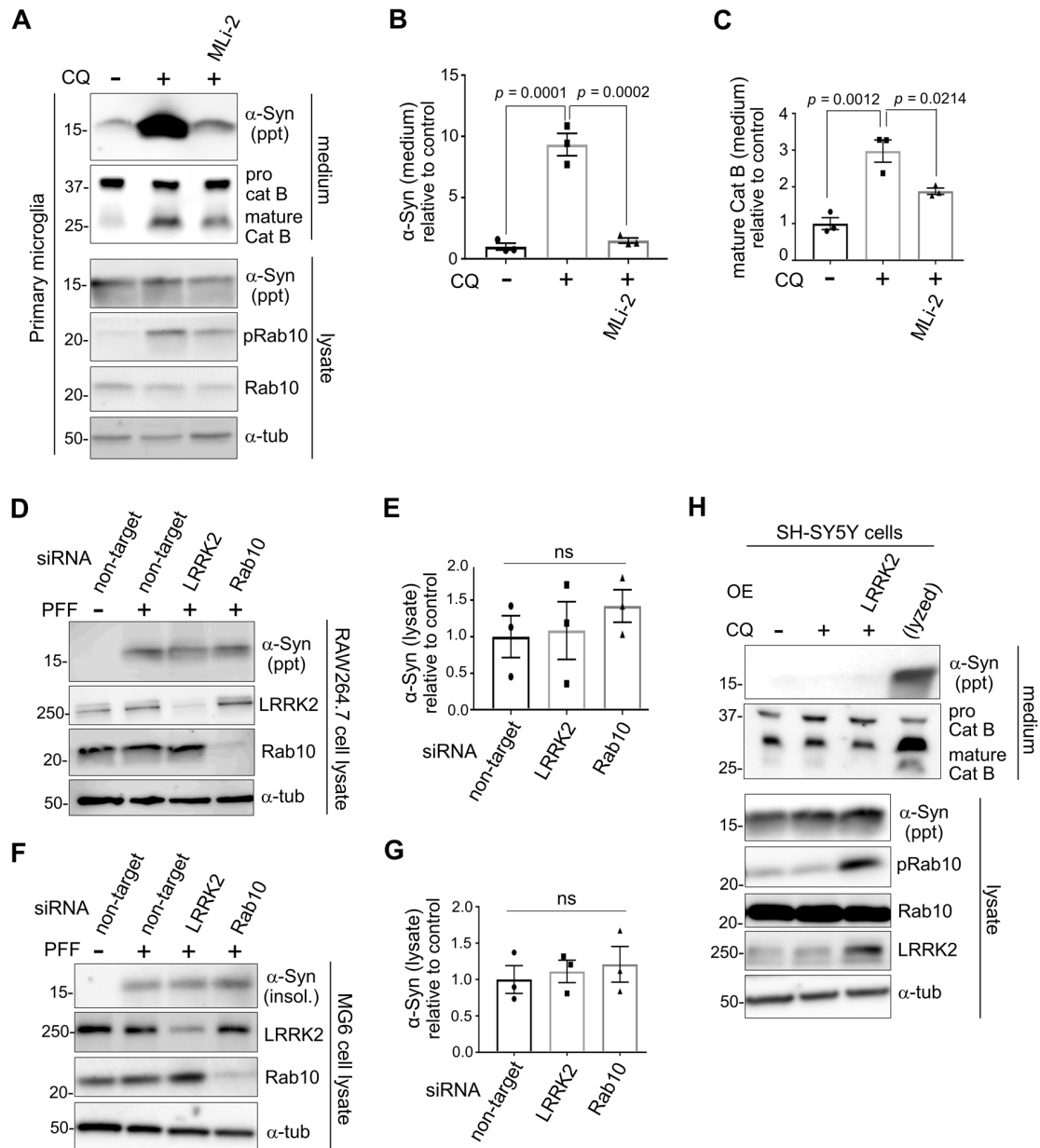


Figure S4. The effect of LRRK2 and Rab10 on the uptake and release of insoluble α -synuclein, related to Figure 4.

(A-C) Inhibitory effect of a LRRK2 kinase inhibitor MLI-2 on CQ-induced release of insoluble α -synuclein from mouse primary microglia laden with α -synuclein PFFs. The representative immunoblot pictures of media and lysates (A), as well as densitometric analyses of insoluble α -synuclein (B) and mature cathepsin B (C) in media, are shown. Data represent relative levels compared to CQ (-) sample. Mean \pm SEM, $n = 3$, one-way ANOVA with Tukey's test. **(D-G)** Comparable levels of internalized α -synuclein in RAW264.7 cells (D, E) or MG6 cells (F, G)

pretreated with siRNA for LRRK2 or Rab10 followed by PFF treatment. The levels of LRRK2 and Rab10 were also analyzed to check the knockdown efficiency. Densitometric analyses of the internalized α -synuclein are shown in E and G, where relative levels compared to control siRNA-treated sample are shown. Data represent mean \pm SEM, n = 3, ns: not significant. **(H)** Lack of the release of α -synuclein and mature cathepsin B from SH-SY5Y cells even under overexpression (OE) of LRRK2. Cells transfected with or without LRRK2 were pretreated with α -synuclein PFFs and then treated with CQ. The medium from cells incubated with lysis buffer was loaded in the rightmost lane as a positive control.

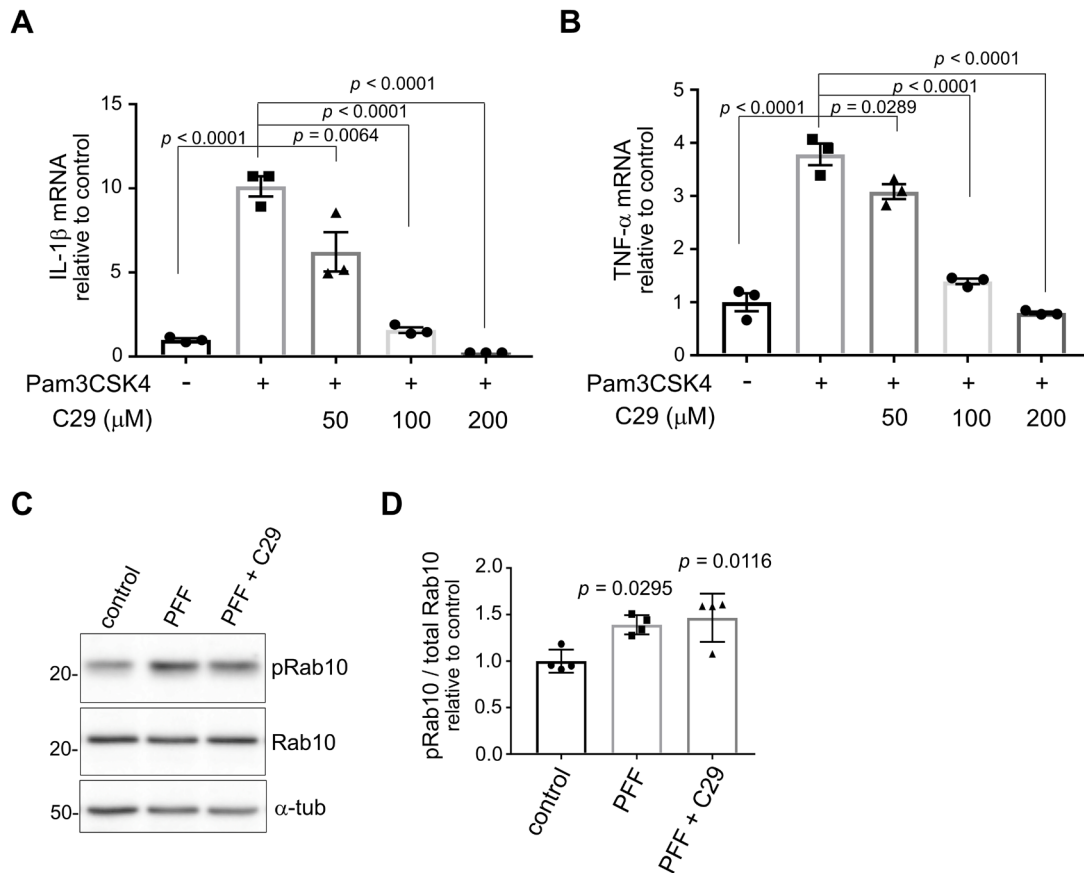


Figure S5. Lack of involvement of TLR2 in Rab10 phosphorylation induction by α -synuclein PFFs, related to Figure 5.

(A, B) Confirmation of inhibitory effect of C29, a TLR2 inhibitor, on TLR2 signaling. mRNA levels of IL-1 β (A) and TNF α (B) in RAW264.7 cells exposed to a TLR1/2 agonist Pam3CSK4 with or without C29 were measured by quantitative RT-PCR. Relative levels compared to control (no treatment) sample are shown. Mean \pm SEM, $n = 3$, one-way ANOVA with Tukey's test. **(C)** Immunoblot analysis of Rab10 phosphorylation in RAW264.7 cells treated with or without α -synuclein PFFs and/or C29 (100 μ M). **(D)** Densitometric analysis of phospho-Rab10 divided by total Rab10, as shown in C. Data represent relative values compared to control (PBS-treated) sample. Mean \pm SEM, $n = 4$, one-way ANOVA with Tukey's test.

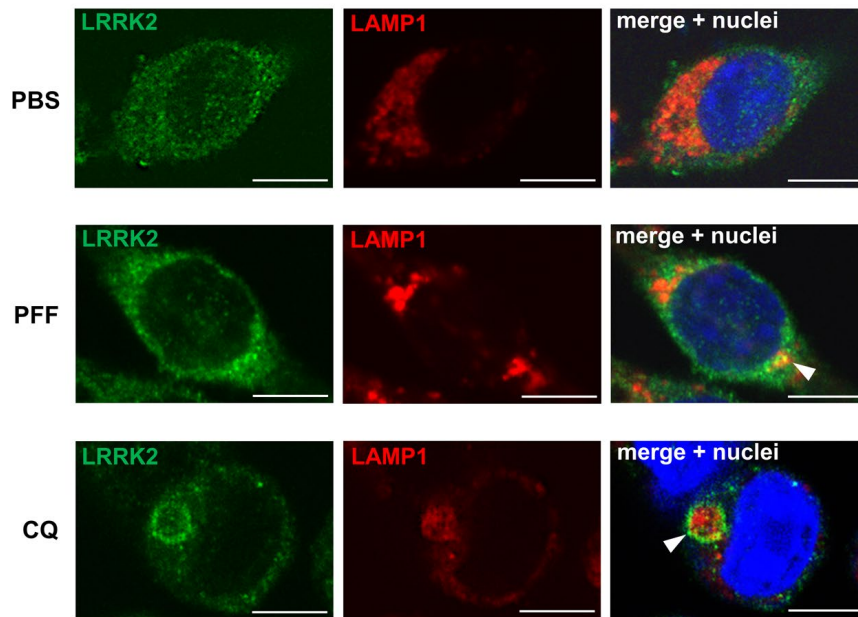


Figure S6. Immunocytochemical analysis of LRRK2 and LAMP1 under exposure to α -synuclein PFFs or CQ, related to Figure 6.

Representative images of immunostaining for endogenous LRRK2 (MJFF2, green) and LAMP1 (red) in RAW264.7 cells exposed to PFFs (for 12 hrs), CQ (for 3 hrs) or PBS (for 12 hrs). Arrowheads indicate the proximal localization of these two proteins that were observed under PFF or CQ exposure. Nuclei were stained with DRAQ5 (blue). Scale bars = 10 μ m.

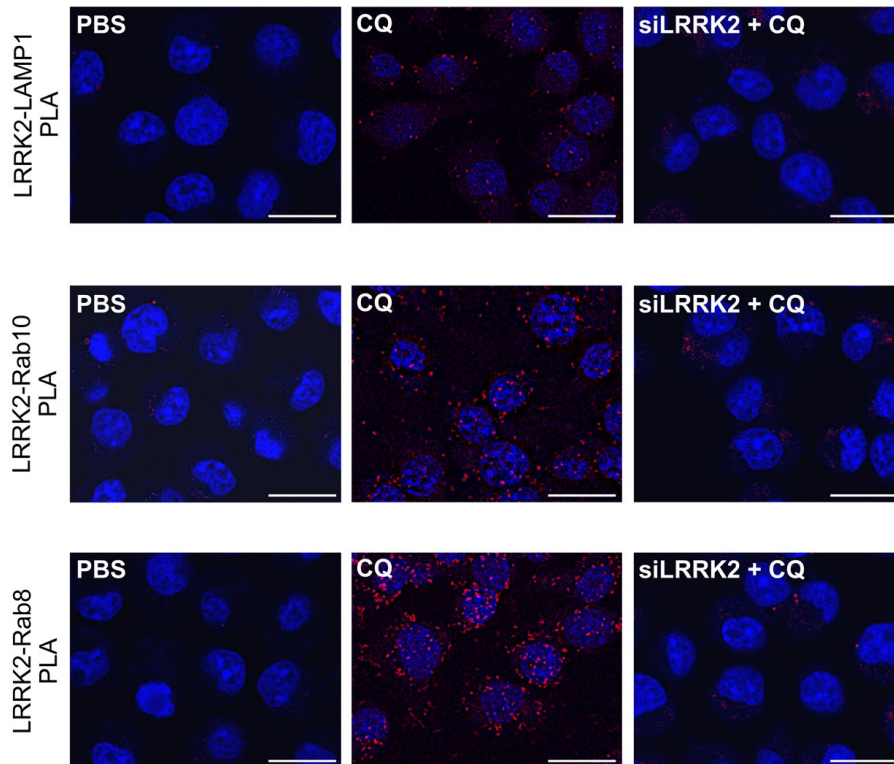


Figure S7. Confirmation of the specificity of proximity ligation (PL) signals, related to Figure 6.

Representative images of PL signals (red) between LAMP1 cytosolic tail and LRRK2 (top), LRRK2 and Rab10 (middle) or LRRK2 and Rab8 (bottom) in RAW264.7 cells pretreated with LRRK2 siRNA (siLRRK2, rightmost panels) or non-target siRNA (middle column) for 48 hrs followed by exposure to CQ or PBS for 3 hrs. PL signals generated by these three combinations were largely diminished under LRRK2 knockdown. Nuclei were stained with DRAQ5 (blue). Scale bars = 20 μm .

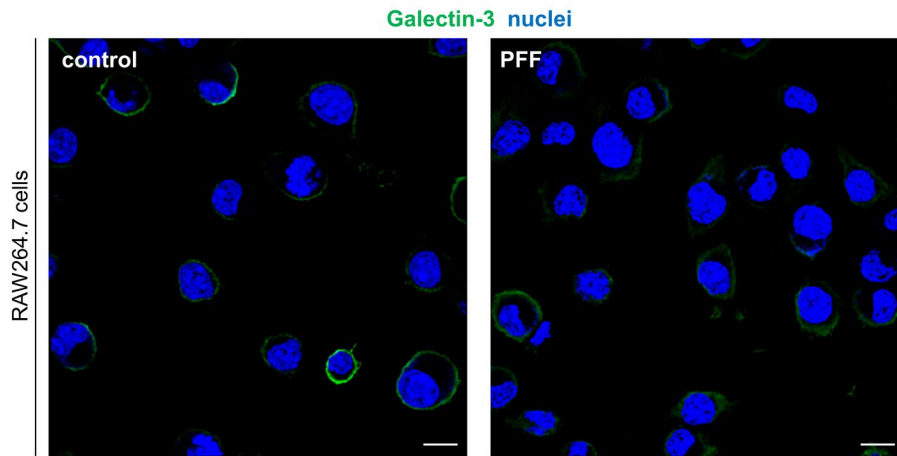


Figure S8. Lack of evidence of lysosomal membrane damage as a downstream event of α -synuclein PFF treatment, related to Figure 6.

Representative images of immunostaining for the membrane injury marker galectin-3 (green) in RAW264.7 cells. Nuclei were stained with DRAQ5 (blue). Scale bars = 10 μ m.